



# IMPLANTOLOGIE

DIE ZEITSCHRIFT FÜR DIE PRAXIS

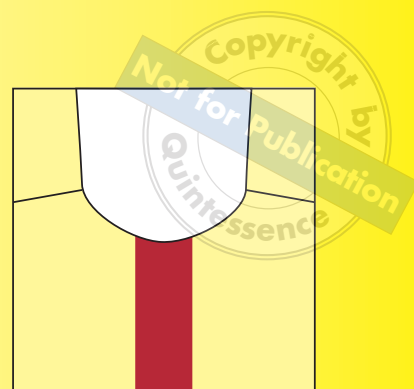
SPECIAL REPRINT

**Application of the synthetic nanostructured bone grafting material NanoBone® in sinus floor elevation**

Jens Meier, Eduard Wolf,  
Volker Bienengraber

VOLUME 16  
SEPTEMBER 2008

**3/08**







Jens Meier, Eduard Wolf, Volker Bienengraber

# Application of the synthetic nanostructured bone grafting material NanoBone® in sinus floor elevation



**Jens Meier**  
Dr. med. Dr. med. dent.  
Practice for oral, maxillary  
and facial surgery  
Bürgermeister-Smidt-Straße 86  
27568 Bremerhaven

**Eduard Wolf**  
Prof. Dr. med.  
Institute of pathology  
Dres. Tiemann and  
Feyerabend a. P.  
Postfach 540 649  
22506 Hamburg

**Volker Bienengraber**  
Prof. Dr. med. Dr. med. dent.  
Functional area  
Experimental research  
Clinic for oral, maxillary and  
plastic facial surgery  
University of Rostock  
Stempelstraße 13  
18057 Rostock

Please address  
correspondence to  
Dr. Dr. Jens Meier.  
E-Mail: ddrjens.meier\_mkg  
@t-online.de

**INDIZES** *Augmentation, hard tissue cutting-grinding technique, histomorphometry, bone grafting material, bone substitutes, NanoBone, nanocrystallites, sinus floor elevation*

This prospective study evaluated the structural changes (modeling and remodeling) as well as the biodegradation of the new bone grafting material NanoBone® based on clinical and histological investigation. Sinus floor elevations were performed on 17 patients using a two-stage protocol when the subantral bone height was less than 5 mm. 43 bone biopsies were collected during implant placement, which was carried out after healing periods of 8–11 weeks (group I) or 12–15 weeks (group II), and subjected to undecalcified tissue processing by applying a hard specimen cutting-grinding technique. The clinical findings showed a solid ossification with bone qualities of D1 or D2, that could be verified in the histologic sections showing impressive hyperostosis. The resorption of NanoBone® and the de novo bone formation took place simultaneously similar to the processes following transplantations of autogenous cancellous bone. Compared with other bone substitutes we observed an accelerated organization and new bone formation that after only 3 months yielded a solid bony layer for primary stable implant placement in the augmented maxillary sinus. Early implantation and functional loading stimulates the new bone and prevents a loss of volume.

## Introduction

For evaluating a new bone substitute, in addition to the usually approved criteria and good clinical safety, it is required that the efficacy as an augmentation material be proven by means of fine-tissue studies as well. This prospective study constitutes a part of the clinical investigations to this effect. The data gained will be discussed compared with other bone substitutes, particular attention being turned to the degree of new bone formation and the progress in time. NanoBone® (Artoss, Rostock, Germany) is fully synthetic, consists of nanocrystalline hydroxyapatite (HA)

mounted in a highly porous silicon dioxide gel matrix and is used in the form of granulates (diameter: 0,6 x 2,0 or 1,0 x 2,0 mm). It is not a sintered ceramic like many other synthetic bone substitutes.

The surface enlarged to maximum on account of the nanostructure sets the stage for a faster adsorption of cells and matrix proteins. The high porosity with an inside surface of 80m<sup>2</sup> per gram<sup>1</sup> favors the invasion of osteogenic cells and of capillary buds as the basis of osseous regeneration.

First the silica gel is replaced by non collagenous matrix proteins within approximately two weeks in vivo<sup>1</sup>. Animal experiments also show a remarkably

**Manuscript**  
Received: July 09, 2007  
Accepted: April 16, 2008

faster new bone formation compared to other synthetic or bovine bone substitutes.

This was confirmed in an upstream human study in which the new bone formation five months after the implantation of NanoBone® in the maxillary sinus and in cystic defects was so impressive that we decided for shorter time windows until taking bone biopsies for this study.

The present prospective study is based on the clinical findings regarding bone quality and the histomorphological evaluation of the biopsy material after augmentation of the caudal maxillary sinus with NanoBone® in relation to time. 17 patients (9 male, 8 female) were included in whom an open sinus floor elevation according to Tatum<sup>2</sup> or Boyne and James<sup>3</sup> was performed because of too little subantral bone height. We drew the line for the indication of two-stage procedures at less than 5 mm.

Five of these patients underwent bilateral augmentation; on one side pure NanoBone®, on the other side NanoBone® with addition of autogenous bone chips was used.

The time windows for taking the bone biopsies were defined that the second stage procedure was performed either eight to eleven weeks (group 1) or twelve to fifteen weeks (group 2) after the augmentation with NanoBone®. The patients were randomly assigned to the groups: eight patients were assigned to group 1 and nine patients to group 2. This should allow for a differentiation in histomorphometry according to time.

## ■ Materials and Methods

### ■ Clinical Procedures

Performing open sinus floor elevations the area of the caudal maxillary sinus was prepared in the typical way and then filled with a mixture of NanoBone® and blood at the ratio of 3:2 (e. g. 1.2 ml NanoBone® plus 0.8 ml venous blood). For those five patients who underwent bilateral surgery, autogenous bone from a bone collector (BoneTrap®; Astra-Tech, Mölndal, Sweden) was added to this material, this portion accounting for approx. 50% of the volume of NanoBone®, that is about a third of the overall volume.

The facial window was not closed separately but only covered with the local periosteum. Preoperatively a one-shot dose of antibiotics using a broad-spectrum cephalosporine was injected. The sutures were removed ten days after the operation. The implantations were performed after eight to eleven and twelve to fifteen weeks and the bone biopsies for histological analysis were taken simultaneously.

The bone biopsies were collected using a trephine bur of an outside diameter of 3.5 mm (Ustomed, Tuttlingen, Germany) which provided a diameter of 3.1 mm for the drilled bone cores. This ensured a sufficient cross-sectional area for the representative analysis of the bone structures. The definite preparation of the implant bed could be performed with small additional effort. Considering the extreme bone density in some cases an intermittent approach was important to avoid heat-necrosis since cooling was possible only at the surface of the trephine bur and on the outside of the bone using physiological saline solution.

### ■ Tissue processing / histology

The bone cylinders were fixed in 10 % formalin solution with 0.1 molar phosphate buffer. The undecalcified cylinders were mounted in methyl methacrylate (Technovit® 9100 new; Kulzer, Wehrheim, Germany)<sup>4,5</sup> and could be prepared using both the hard tissue cutting technique for histologic evaluation (rotation microtome; Leica company, Solms, Germany)<sup>6,7</sup> and the separating thin grinding technique<sup>8,9</sup> (separating and grinding machines, Exakt company, Norderstedt, Germany) up to a layer thickness of 20 to 30 µm. Then they were deacrylated and stained using haematoxylin-eosin, toluidine blue according to Giemsa, Goldner- and von Kossa-staining and / or processed further for immunohistology / histochemistry (tab. 1).

Histological evaluation and photo documentation were performed using the Axioplan 2 Imaging® microscope (Carl Zeiss company, Göttingen, Germany). Histomorphometry was carried out after digitalization using the MosaiX software, AxioVision 4.3 with the image processing software analySIS 5.0 (Soft Image Systems company, Münster, Germany).

The international standard definitions for histomorphometry of bones were used<sup>10</sup>:

1. *Total area of cross-section* = bone / spongiosa with total medullary space (with and without NanoBone®): TiAr = Tissue Area in mm<sup>2</sup>;
  2. *Bone area*: Mineralized and non mineralized bone tissue: BoAr = Bone Area in mm<sup>2</sup>;
  3. *Medullary space without NanoBone®*: Intertrabecular area of the medullary space: BmAr = Bone Marrow Area in mm<sup>2</sup>;
  4. The *cross-sectional area of NanoBone®* in mm<sup>2</sup> was registered as NB.
- Those sections of the drill cores coming from the original alveolar process were examined separately from the augmented areas. The measurement is based on Merz' grids<sup>11</sup> and requires a cross-sectional area of > 20 mm<sup>2</sup> with 160- to 200-fold magnification with more than 50 segments. Compressed or strongly disintegrated biopsies were excluded from this study.

**Table 1** Data on the Processing Methods

Method	Product	Manufacturer	Test
<b>Plastic embedding</b>			
Polymethyl methacrylate	Technovit® 9100 NEW4	Heraeus Kulzer, Wehrheim/Taunus	Polymerization system in the cold for the embedding of mineralized tissue. Undecalcified processing using hard tissue cutting and separating thin grinding technique in histology, immuno- and enzyme histochemistry and in-situ hybridization.
<b>Stainings</b>			
<i>Hard tissue cutting</i>			
HE	Burkhardt <sup>6</sup> , Schenk <sup>7</sup> Haematoxylin-eosin		General staining
Tb-G	Toluidine blue -Giemsa		Visualization of the cellular components
MG	Trichrome staining acc. to Masson-Goldner		Mineralized substance green, osteoid red
<i>Grinding preparations</i>			
Tb	Donath <sup>8</sup> Toluidine blue		General staining for the ground section, visualization of the cellular components
<i>Immunohistology (IH)</i>			
ICH	AK: CD34, clone: QBEnd-10 # M7165	DakoCytomation (Glostrup, Denmark)	Endothelial cells (capillaries)
ICH	AK: CD45(LCA), clone: 2B11 + PD7/26 #M0701	DakoCytomation (Glostrup, Denmark)	Leucocytes common antigen; reacts with all isotypes of the CD4 family
ICH	AK: CD68, clone: PG-M1 #M0876	DakoCytomation (Glostrup, Denmark)	Cells of the mono- and macrophagocytic cell lines; Osteoclasts, mast cells
ICH	AK: VS38c, clone: VS38c #M7077	DakoCytomation (Glostrup, Denmark)	Anti p63 protein; plasma cells, epithelial cells, undifferentiated also in spindle cells and osteoblasts, osteoblastic precursor cells, monocytes, neutrophilic lymphocytes
<i>Detection system for immunohistology (DS)</i>			
DS	StreptABComplex/AP #K0391	DakoCytomation (Glostrup, Denmark)	Complex consisting of streptavidin, coupled with alkaline phosphatase
DS	Rabbit anti mouse/biotin #E0413	DakoCytomation (Glostrup, Denmark)	Secondary / bridge antibody biotin, coupled for immunohistological detection procedures
DS	Goat anti rabbit/ biotin #E0432	DakoCytomation (Glostrup, Denmark)	Secondary / bridge antibody biotin, coupled for immunohistological detection procedures
DS	Pararosaniline #107509	Merck, Darmstadt	Chromogen for enzyme detection, reddish brown
<i>Histochemistry (HC)</i>			
ASD	Naphtol AS-D-chloroacetate #29995	Serva, Heidelberg	Substrate for ASD-chloroacetate esterase detection for granulocytes, different levels of maturation and mast cells

## ■ Results

### ■ Clinics

17 patients who underwent surgery according to the study design were included. Nine were male and eight female of an average age of 55.2 years (m: 56.2; f: 54.8).

The healing periods of eight to fifteen weeks were shorter than the recommended healing periods for other bone substitutes.

Bego-Semados S-implants (Bego-Implant Systems, Bremen, Germany) and Astra-Tech-implants (Astra-Tech, Mölndal, Sweden) were inserted and definitive prosthetic work and functional loading started ten to twelve weeks post implantation. None of the 43 implants placed in the augmented area was lost during the observation period (key date 31 January 2008); incorporation time ranged from 19 and 33 months.

No bone loss was found in the clinical appearance or in the radiological follow-up x-rays.

While bone qualities of D3 or D4 are common in the lateral maxilla in particular in the former molar area<sup>12</sup>, we have regularly found very firm i.e. D1- or D2-bone above the residual alveolar process when using the trephine burs and preparing the definitive implant bed as well as when screwing in the implants. Only one female patient (78 years of age, smoker, no drug history) showed D3 bone during implant insertion, which however was not important given the possible implant length of 13 mm.

### ■ Histology

When taking the bone biopsies, we managed without difficulty to gain a long bone cylinder (Fig. 1a), when the newly created maxillary sinus floor was directly above the end of the trephine. From time to time the drill cores remained firmly linked with the augmented area through the small base of the cylinder and had to be prepared separately which was difficult because of the density of the bone and on the other hand on account of the necessity not to extend the future implant bed. Some predrilled cylinders could only be extracted in several segments (Fig. 1b), so that only sections shorter than the bone cores of ideally more than 10 mm could be examined.

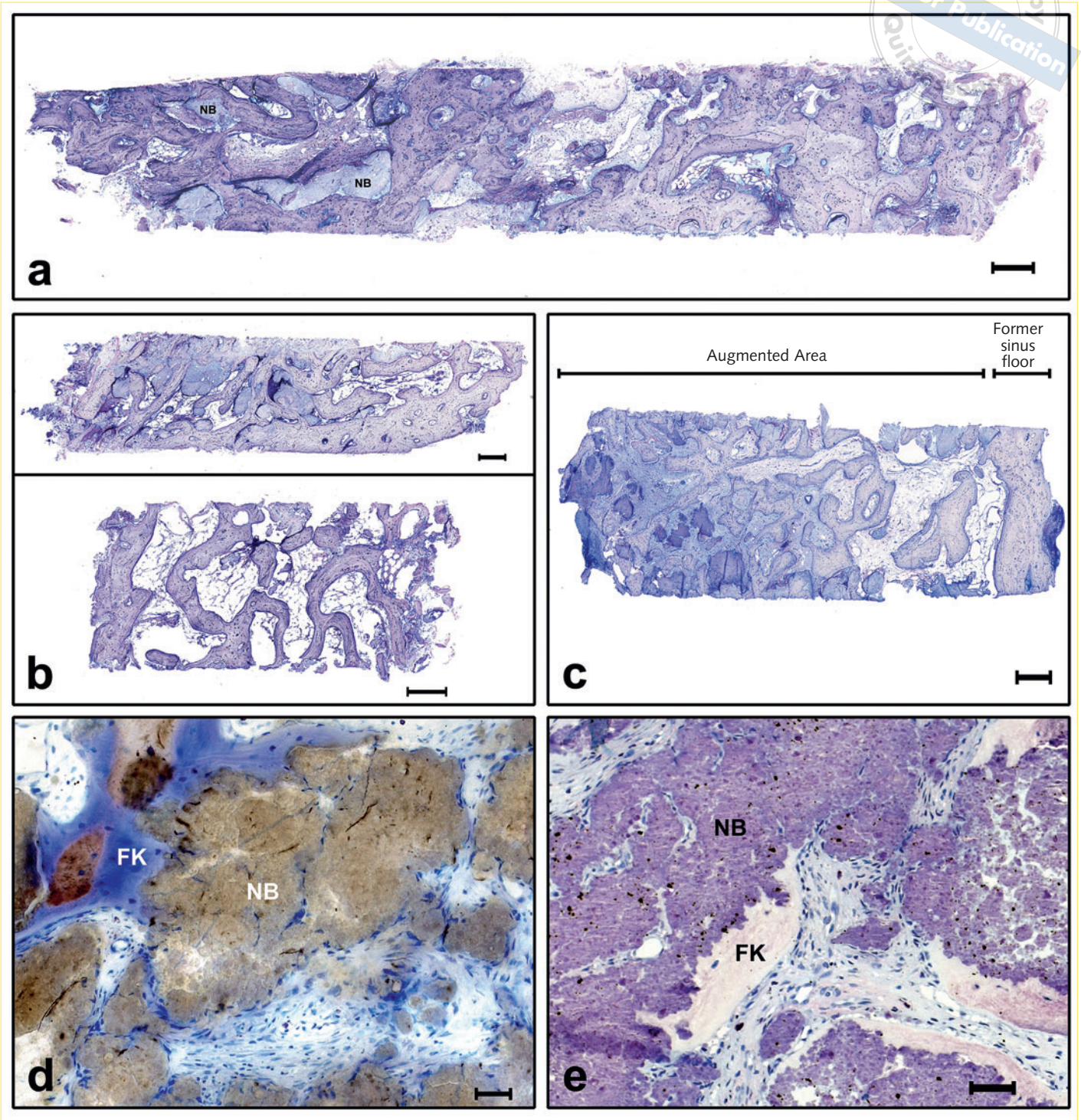
When no well-preserved bone structure was gained or the samples were excessively segmented only morphological but no histomorphometrical analyses of these biopsies could be performed. Thus 25 out of the 43 biopsies remained for quantitative evaluation. The numbers in table 2 refer to the consecutive numbering of the samples. Bone cylinders of the original alveolar process without squeezing artifacts were obtained in five samples only all others were excluded from the histomorphometrical examination due to the irregular structure which had been created by pressing out fat marrow and the disturbance of the trabecular architecture when removing it from the trephine burs.

The augmented bone tissue showed signs of hyperostosis in the form of broad, plump trabeculi that consisted of woven bone in the early stages. Residual NanoBone® was found enclosed in de novo bone formations (Fig. 1a to c). The contact zone between the osteoblasts and the bone substitute showed a large amount of osteoid (Fig. 2b to d) which partly infiltrated the NanoBone® particles. Furthermore cellular resorption by osteoclasts and macrophages is observed on the surface of the NanoBone® particles.

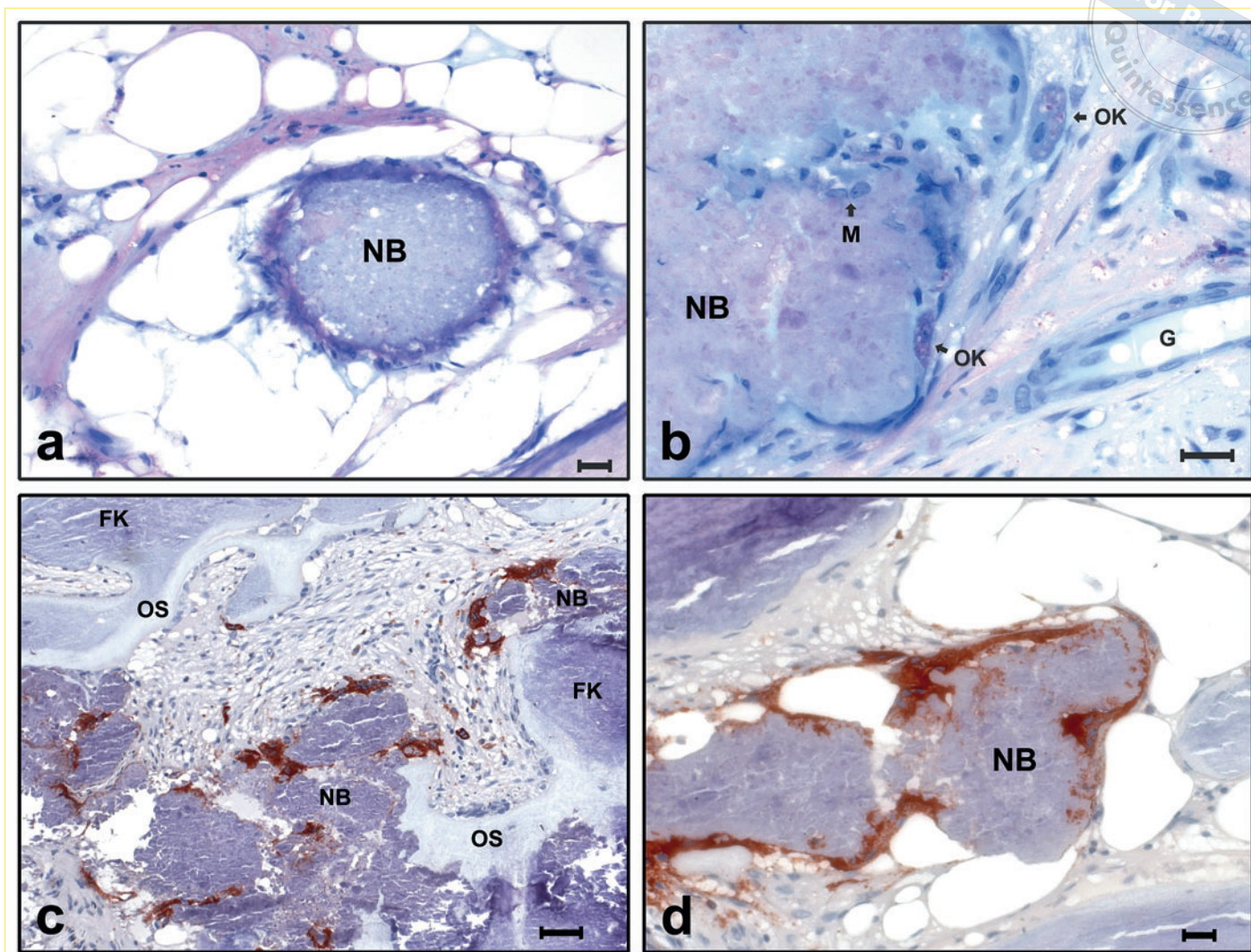
A dense osteoblast lining with increased activity and broadening of the trabeculi's diameter was found in the adjacent local bone as a result of the endosseous stimulation (Fig. 1b at the bottom). After longer healing periods hyperostosis increased as well in the bone as in the augmentation material (Fig. 1c).

Table 2 gives an overview of the variety of the findings. First of all the average portion of the bone area of 37.7% in the augmentation material exceeds the one in the local alveolar process by 3%. The predominantly incorporated NanoBone® portion (NB) of an average of 19.3% adds to that figure which explains the remarkable increase in the bone density. The part of the medullary space is reduced and now amounts to an average of 43% which is approximately one third less than in the local alveolar process with 66.1% in average.

The volume of NanoBone® in the total cross section reduces in time which can be demonstrated in samples taken after prolonged periods. When NanoBone® is mixed with blood in the recommended ratio of 3 : 2 in volume the histomorphometrical analysis yielded 39.7% NB and 60.3% for the coagulum.



**Fig. 1a to e** Microscopic images of biopsy material in histological cutting and grinding preparation. **a** Overall image of a 9.6-week-old bone cylinder regio 14. It shows augmented bone tissue and enclosed small residual NanoBone® particles (NB), scale: 500 µm; hard tissue cut; toluidine blue Giemsa staining. **b** Overall image of a bone cylinder regio 17 from the same patient as described under 1a, scale: 500 µm; hard tissue cut; toluidine blue Giemsa staining. **c** Overall image of a bone cylinder after augmentation regio 25 14.1 weeks after NB implantation. Augmented bone tissue with NB particles and residues of the local maxillary sinus bone (KH) are visualized, scale: 500 µm; hard tissue cut; toluidine blue Giemsa staining. **d** Sectional enlargement of a bone cylinder (separating thin grinding preparation, approx. 10 µm thick). Almost completely enclosed small NanoBone® particles (NB) can be seen in the woven bone (FK), scale: 50 µm; toluidine blue Giemsa staining. **e** Hard tissue cut of bone tissue of the same patient as presented under Fig. 1d. scale: 50 µm; toluidine blue Giemsa staining.

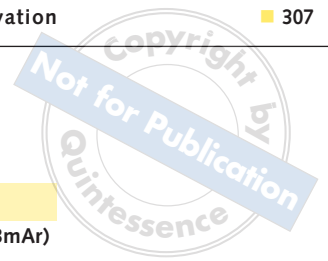


**Fig. 2a to d** Microscopic images of NanoBone® in resorption. **a** NanoBone® particles (NB) after augmentation, 9.6 weeks after implantation. On the surface of the NB particle, resorbing mononuclear cells (macrophages) can be seen. scale: 20 µm; hard tissue cut; toluidine blue Giemsa staining. **b** Sectional enlargement of a NanoBone® particle (NB) in resorption and degradation with infiltration of resorbing mononuclear cells (macrophages = M) into the NB particle. At the surface multinuclear osteoclasts (OK) and an accompanying reticular vascular connective tissue (G). scale: 20 µm; hard tissue cut; toluidine blue Giemsa staining. **c** Status after augmentation with NanoBone® (NB). NB particles with newly formed trabecular woven bone (FK) and fibrous osteoid (OS) as well as multinuclear osteoclasts (stained in red) indicating resorption. scale: 50 µm; hard tissue cut with immunohistological visualization of CD68. **d** Detail of Fig. 2c with multi- and mononuclear resorbing osteoclasts (stained in red) at the surface of the NanoBone® particle (NB). scale: 20 µm; hard tissue cut with immunohistological staining by CD68.

Taking into consideration the variation of the measured ratios and the small number of samples analyzed in this study we can only state that the mean compartment of NB in this material has decreased to 19.3% .

The reduction in the NB portion can be explained as the consequence of the degradation of the bone substitute. Only approximately 50% of the initially inserted augmentation material was still present after two to three months.

Because of the high porosity the biodegradation of the NB particles took place simultaneously at the surface and within the interconnecting internal spaces through resorbing mononuclear cells (macrophages and/or histiocytes) that showed a high cell density in the early stages. They promoted the osteoclastic degradation of the NB (Fig. 2a and b). A positive immunohistochemical antigen proof for CD 68 was achieved which is regularly expressed by macrophages and osteoclasts (Fig. 2c and d; Fig. 3c).

**Table 2** Results of the Histomorphometrical Examination after Sinus Floor Elevation (SFE) (n = 25)

<b>Histomorphometrical Measurements: Bone Cylinders after SFE (augmented area)</b>								
Cons. no.	Meas. field (TiAr)		Bone area (BoAr)		Area: NanoBone® (NB)		Area: medullary space (BmAr)	
	mm <sup>2</sup>	%	mm <sup>2</sup>	%	mm <sup>2</sup>	%	mm <sup>2</sup>	%
1	15.7	100.0	8.4	53.8	3.4	21.4	3.9	24.8
2	20.1	100.0	11.7	58.2	1.8	8.9	6.6	32.9
6	4.8	100.0	2.1	44.5	0.7	14.3	2.0	41.2
8	11.6	100.0	5.3	45.5	1.15	9.9	5.2	44.7
9	11.5	100.0	2.4	20.6	4.5	39.5	4.6	39.9
10	13.5	100.0	7.2	52.9	0.9	6.8	5.4	40.2
11	10.9	100.0	4.3	39.5	4.0	36.5	2.6	24.0
12	4.8	100.0	0.7	14.3	1.3	27.5	2.8	58.1
13	16.7	100.0	6.7	40.1	1.9	11.4	8.0	47.9
14	13.2	100.0	6.4	48.6	2.7	20.5	4.1	30.9
20	7.1	100.0	1.7	23.9	2.0	28.2	3.4	47.9
24	18.0	100.0	8.3	46.1	1.2	6.6	8.5	47.3
25	11.2	100.0	3.0	26.9	4.2	37.8	4.0	35.3
28	4.9	100.0	2.1	42.3	1.4	29.3	1.4	28.4
29	19.0	100.0	6.7	35.2	3.4	17.7	8.9	47.1
30	15.8	100.0	5.1	32.6	1.6	10.0	9.0	57.4
31	4.9	100.0	1.7	34.4	0.2	4.9	3.0	60.7
32	10.2	100.0	3.7	36.5	0.4	3.7	6.1	59.8
33	18.9	100.0	9.8	51.9	2.1	11.1	7.0	36.9
34	17.8	100.0	3.9	21.9	2.7	15.3	11.2	62.8
36	5.5	100.0	1.1	19.3	1.5	28.3	2.9	52.4
37	8.9	100.0	3.6	39.8	1.4	15.4	4.0	44.8
40	11.7	100.0	4.7	40.3	4.0	33.9	3.0	25.8
41	20.7	100.0	7.7	37.2	5.2	25.1	7.8	37.7
43	12.7	100.0	4.5	35.8	2.3	18.0	5.8	46.2
<b>Mean</b>	12.4		4.9	37.7	2.2	19.3	5.2	43.0
<b>Median</b>	11.7		4.5	39.5	1.9	17.7	4.6	44.7
<b>SD</b>	5.1		2.8	11.4	1.3	10.7	2.5	11.3
<b>Histomorphometrical Measurement: Bone Cylinders – local Bone (without NB)</b>								
Cons. no.	Meas. field (TiAr)		Bone area (BoAr)		Area: medullary space (BmAr)			
	mm <sup>2</sup>	%	mm <sup>2</sup>	%	mm <sup>2</sup>	%		
1	8.8	100.0	4.0	45.6			4.8	54.4
6	5.8	100.0	1.7	29.0			4.1	71.0
9	7.8	100.0	2.7	34.1			5.1	65.9
12	9.9	100.0	3.4	33.9			6.5	66.1
36	8.1	100.0	2.5	30.9			5.6	69.1
<b>Mean</b>	8.1		2.8	34.7			5.2	65.3
<b>Median</b>	8.1		2.7	33.9			5.1	66.1
<b>SD</b>	1.3		0.8	5.8			0.8	5.8
<b>Histomorphometrical Measurement: Reference 0 – NanoBone® in Blood</b>								
					Area % NB		Area % BmAr	
<b>Mean</b>					39.7		60.3	

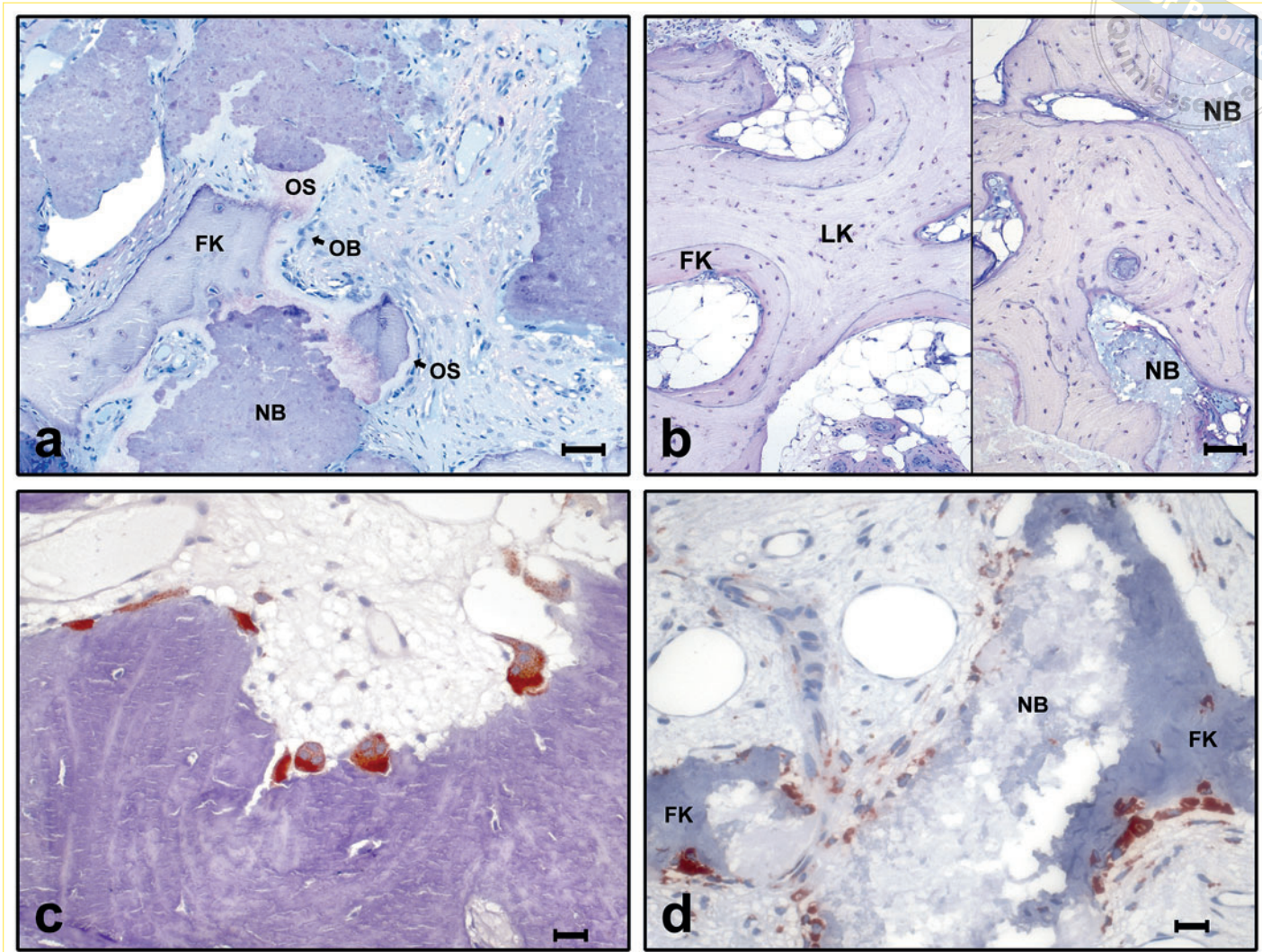


**Fig. 3a to d** Microscopic images of modeling and remodeling. **a** Status 14.1 weeks after NanoBone® implantation (NB) in regio 25. Newly formed trabecular woven bone (FK) with broad osteoid borders and osteoblast lining (OB) can be seen. The NB particles show direct contact zones with the osteoid (OS). scale: 50 µm; hard tissue cut; toluidine blue Giemsa staining. **b** Details of the patient (right maxilla) 9.6 weeks after augmentation with NanoBone® (NB) and autologous bone chips. On the left: local bone with clear signs of the endosteal remodeling that has taken place with formation of cement lines, central lamellar bone (LK) and apposition of woven bone (FK). On the right: Analogical findings: Enclosed NB particles with direct contact to the newly formed bone. Scale: 100 µm; hard tissue cut; toluidine blue Giemsa staining. **c** Status 13.9 weeks after the implantation of NanoBone® and autologous bone chips. In the immunohistological evidence newly formed woven bone with mono- and multinuclear osteoclasts (stained in red) can be seen on the surface of the remodelling bone, scale: 20 µm; hard tissue cut with immunohistological visualization with CD 68. **d** Immunohistological visualization with Vs38c on the same biopsy material as in Fig. 3c. Resorptive processes at the degrading NanoBone® (NB) with strong disintegration of the NB particles while cubic and flat osteoblasts can be seen on the surface of the woven bone scale: 20 µm; hard tissue cut with immunohistological evidence, (antigen demasking with microwave pretreatment). Vs38.

Figures 3a to d show typical findings after about ten weeks: The newly formed woven bone is covered by a continuous layer of flat osteoblasts; the highly active osteoblasts are rather prismatic and have produced broad osteoid bands which create bridges between the NanoBone® particles and have been transformed into woven bone due to mineralization (Fig. 3a).

The remodeling into lamellar bone has already taken place which is shown by the Haversian systems, cement lines, mature osteocytes and the loose connective tissue of the reticular marrow (Fig. 3b). Indicating resorption in the process of remodeling mono- and multinuclear osteoclasts are not only found on the NanoBone® surface but also on the newly formed bone (Fig. 3c).

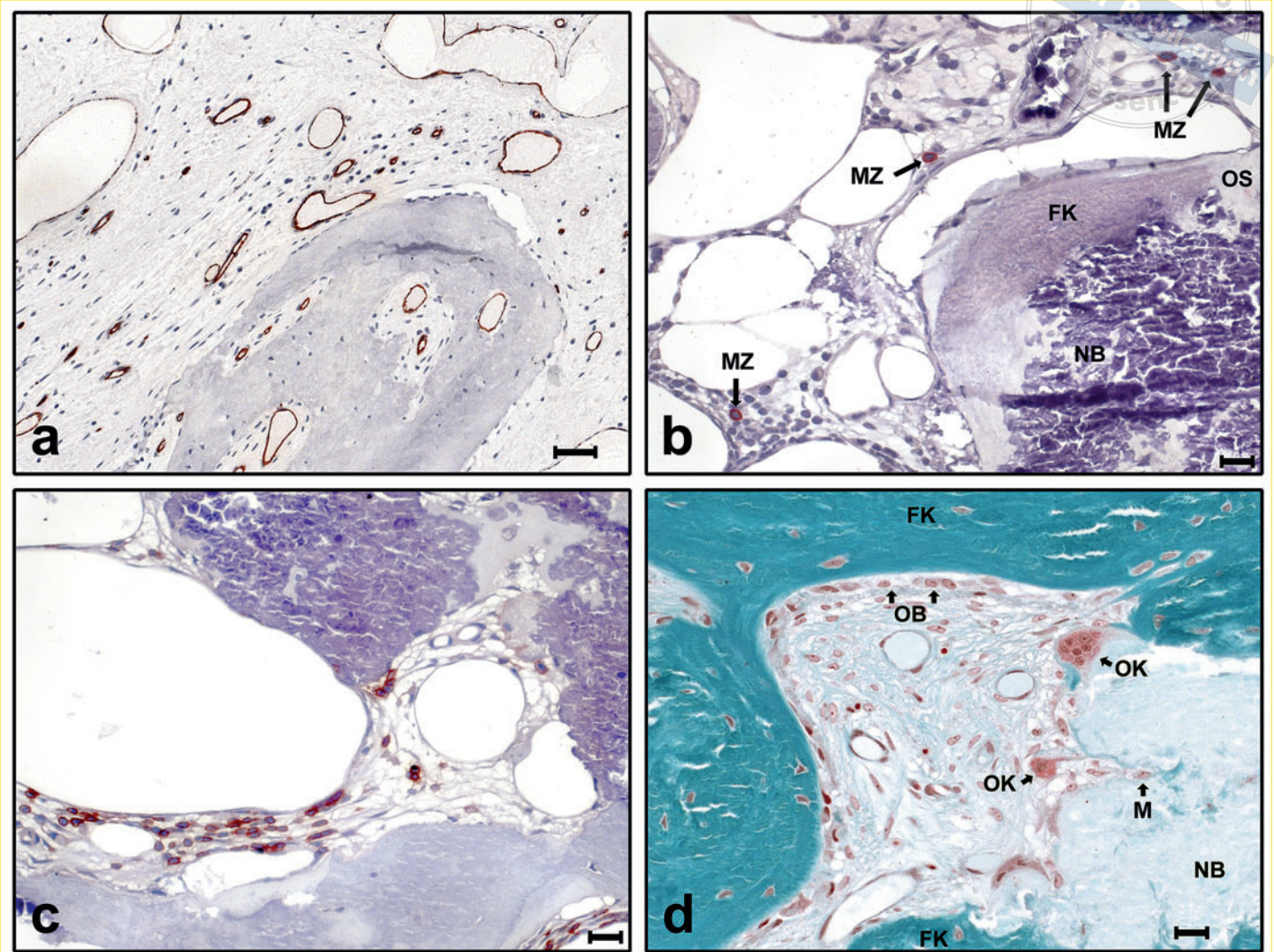


**Fig. 4a to d** Microscopic images of cellular activity. **a** Immunohistological determination of the vessels with CD34 (red; antigen demasking with microwave pretreatment). Newly formed woven bone in the reticular vascularized connective tissue as well as vascular sections can be seen in the intertrabecular space, scale: 50  $\mu$ m; hard tissue cut. **b** NanoBone® particle (NB) in contact with woven bone (FK) and/or with osteoid (OS). Histochemical determination of mast cells (MZ) with ASD chloracetate esterase (red cytoplasm) in the adjacent loose reticular abundant capillaries containing connective tissue, scale: 20  $\mu$ m; hard tissue cut. **c** Additional detail from 4b: Cells in the intertrabecular connective tissue. The lymphocyte population is identified red in the immunohistological determination with CD45/LCA, scale: 20  $\mu$ m; hard tissue cut. **d** Detail of a hard tissue cut, using trichrome staining according to Masson-Goldner. At the bottom on the right a NanoBone® particle (NB) is visible in contact with woven bone (FK) and shows multi- and mononuclear osteoclasts (OK) as well as degrading mononuclear cells (M) on the surface. The mineralized bone tissue is stained green with cubic osteoblasts (OB) on the surface. The space in between is filled with reticular connective tissue, scale: 20  $\mu$ m.

The osteoblast lining is present on the NanoBone® surface and on the woven bone. The immunohistological detection is achieved using the antibody Vs 38c (Fig. 3d). The width of the osteoid area in combination with the cell height can be assessed as an expression of the activity of the osteoblasts.

Figure 4a shows abundant capillaries and angioblasts (= capillary buds marked cells without lumen)

identified by CD 34 as endothelial cell marker. The presence of lymphocytes and mast cells that are marked by CD 45 (LCA) (Fig. 4b and c) in addition to osteoblasts and osteoclasts (Fig. 4d) is a typical sign for regeneration and corresponds to the picture of physiological periosteal bone formation during the growth period and undisturbed healing of bone fractures<sup>13,14</sup>.

None of the samples showed inflammatory infiltrates or foreign-body reaction or a tight collagenous and poorly vascularized fiber formation like scar tissue or fibrous enclosure.

## ■ Discussion

The generally accepted standards for bone substitutes and / or grafting materials include:

- no transmission of infections or other diseases
- absence of allergizing components
- good applicability
- sufficient volume stability
- osteoconductivity
- complete resorbability with simultaneous replacement by vital lamellar bone and
- possibly an osteoinductive potential.

The material examined in this study meets these criteria. The first two requirements are met through the synthetic origin and the use of nature-identical components (HA and SiO<sub>2</sub>). A good applicability is achieved by mixing it with venous blood (or blood collected from the site of augmentation) in the given mixing ratio which results in a well moldable compound.

The augmentation material's volume stability depends decisively on the resorption period and the new bone formation which under ideal conditions takes place simultaneously. The functional stimulus by the early loading of the implants after only a relatively short integration period is decisive for volume preservation. This prevents inactivity involution that has been observed after augmentation with autogenous bone and long incorporation periods<sup>5,28</sup>. This observation lead to the recommendation of performing an overcompensation by approx. 30% in those cases. Because of the inconstant resorption of excessive autogenous bone this is not necessary at all if the functional loading takes place early and in accordance with bone physiology.

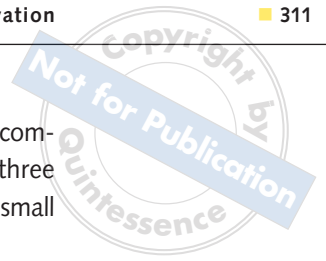
For NanoBone® complete resorption can be expected after approximately nine months (unpublished author's data). During this period, the residual volume of NanoBone® falls below 10% and new vital bone is formed. After the initial period with formation of woven bone, the transformation into lamellar bone starts from the forth week on and the function-oriented structured remodeling begins after another eight to twelve weeks in case of prompt (after eight to twelve weeks) implantation and functional loading of the implants.

No loss of marginal or antral bone height was observed during the follow-up period of at least eighteen months. This is confirmed by the findings of recall examinations and survey radiographs. Radiographic findings are only suitable for volume determination but not for the assessment of the resorption progress or new bone formation since the NanoBone®-blood mixture and the regenerated bone do not really differ from natural bone on account of the grain size and the calcium content.

All histological preparations show the good osteoconductivity since the NanoBone® particles are in close contact with the appositionally formed new bone and/or are enclosed in bone. The cellular colonization of the inside and outer surfaces and the early and considerable vascularization are decisive for appositional osteogenesis. Similar to the healing of bone fractures the immobilization of the augmentation material is mandatory. This can easily be achieved in the maxillary sinus, at other sites this has to be demanded as *conditiosine qua non* and where necessary to be ensured through a suitable coverage<sup>15</sup>.

It is under discussion whether NanoBone® can be considered to have an osteoinductive potential. Further studies will be carried out on this subject to settle this question, but this is not part of this study. Nevertheless, the histological findings with a new bone formation that is found constantly throughout the entire cross section of the samples – not only "creeping substitution" from the neighbouring bone like other bone substitutes – suggest such presumptions.

The principles for the filling of osseous defects with autogenous bone transplants are standard methods and references for the use of bone substitutes in combination with implant therapy. Their main inconvenience consists of the donor-site morbidity and the possibly limited availability. Nevertheless, the comparison of the cellular processes in the transplantation of autogenous bone provides interesting parallelities to the augmentation using bone substitutes since the cascade of cellular reaction recurs everywhere. A characteristic feature of both the



transplantation of autogenous bone blocks and of particulate bone tissue reveals the fact that regeneration takes place starting from the adjacent bone by "creeping substitution" and also as new bone tissue is formed in the wake of vascularization with the resorption of the transplanted bone taking place simultaneously. The same happens in case of the augmentation using NanoBone® with the analogous sequence of cellular reactions like that after the transplantation of autogenous cancellous bone.

The vascularized adjacent tissue always is the starting point of the regeneration processes. Comparing NanoBone® with other bone substitutes different features can be observed with regard to the penetration of the augmentation material with macrophages and newly formed blood-vessels. This angiogenic new bone formation was described by Röser et al.<sup>29</sup> for the augmentation with hydroxyapatite. Transplants made of cancellous bone blocks are ossified within three to four months, transplants mainly made of cortical blocks need nine to twelve months for complete osseous integration. A healing period corresponding to the latter (six to twelve months) is recommended for coralline bone substitute<sup>19</sup>,  $\beta$ -TCP<sup>20,28</sup> and bovine bone matrix<sup>21,26,27</sup>.

In all cases new bone formation only takes place starting from the border (creeping substitution).

Therefore, the angiogenic osteogenesis taking place throughout the entire volume in NanoBone® constitutes a true difference in quality. The comparison with the regeneration periods of other bone substitutes emphasizes the essentially faster new bone formation with NanoBone®: For  $\beta$ -TCP (e. g. Cerasorb®; Curasan Ltd., Kleinostheim, Germany), an incorporation period of nine to twelve months up to fifteen months is recommended before implantation<sup>18,20,25,28</sup> and a six to twelve months incorporation period is recommended for bone substitutes of bovine origin (e. g. BioOss®; Geistlich, Wolhusen, Switzerland)<sup>21,26,27</sup>; the time until loading of the implants would add another six months.

Only a small number of papers is available in which histomorphometrical data have been published for these bone substitutes after sinus floor elevations. Those show that 17 to 34% of newly formed bone was found eight to twelve months after sinus floor elevations with bovine bone matrix<sup>21,26</sup> and 17 to 38% after implantation of  $\beta$ -TCP<sup>20,28</sup> after similar periods.

After sinus floor elevations with NanoBone® comparable values are available after less than three months. The mean ratios found in this relatively small test group are:

- 37.7% for calcified bone (BoAr)
- 43.0 % for bone narrow (BmAr) and
- 19.3 % for residual NanoBone®

Our data show a considerable standard deviation (SD about 11%). Median values however show little differences:

- 39.5 % BoAr
- 44.7 % BmAr and
- 17.7 % for NB residues.

The relation between calcified bone and bone marrow in the alveolar process only shows a small deviation and is approximately one to two thirds (34% vs. 66%) which corresponds to literature.

The fact that no substantial difference was found in case of addition of autogenous bone (chips from bone collectors) is noteworthy but cannot be evaluated statistically – due to the small test group. The differentiation according to time of the sample collection between group 1 and 2 does not show any reliable differences. This may result from the fact that the times of sampling did not differ much and the interindividual variables obscure possible differences. Studies including a larger number of cases are necessary to answer these questions.

Hydroxyapatite (HA) is the inorganic component of bone. This is why the request for synthetic bone substitutes in the early 80's resulted in the development of different bone substitutes based on HA granules sintered at high-temperatures<sup>30,31</sup>. Its most striking characteristic was the fact that new bone formation was achieved under very special conditions only. In most cases only an invagination by connective tissue and at best the formation of a fibrous scar was seen but most often sequestrations occurred even after several years. For bone substitutes made of  $\beta$ -TCP of similar macrostructure the results are alike although presentations with new bone formation established this material as one of the current references for bone substitutes.

The disturbed, missing or delayed de novo bone formation for sintered hydroxylapatite or tricalcium phosphates can be explained by the lack of porosity

and the poor solubility and/or the lack of phagocytability of the HA macrocrystals. The disadvantage of the lack of porosity was avoided by using coralline or bovine bone substitutes. These preparations also contain HA macrocrystals that are characterized by high stability and the resistance to resorption. This is why remnants of these bone substitutes are still found even after more than two years. Since foreign material in the bone results in bypass structures<sup>32,33</sup> it has to be discussed whether this can be justified for achieving higher stability of the augmented volume or offers functional advantages at all compared to the naturally structured bone<sup>17,18</sup> and has a relevant influence on the long-term success of implants.

After the transplantation of autogenous bone and complete ossification this is of identical biological value like the original bone. The same applies to the status after augmentation with NanoBone®. The stability of the augmented volume here is not the effect of the filler but the functional requirements that are stimulating the bone around implants and natural teeth. Thus the correctly timed functional loading of the implants determine volume as well as the trabecular structure of the new alveolar bone.

The cellular reactions after augmentation of the sinus using NanoBone® correspond to those of primary healing after bone fractures<sup>32,33</sup>. No signs of a resorptive inflammation were found in the study's collective. The cells responsible for osteogenesis are generated by the sessile periosteal and endossal stem cells of the recipient site and of circulating stem cells and by angiogenesis. The latter is responsible for the image of the neo-osteogenesis taking place almost homogeneously throughout the entire cross section.

The nanocrystalline hydroxyapatite embedded in amorphous silica gel leads to a vast enlargement of the internal surface which is attracting the precursors of cellular regeneration through the adsorption of thrombocytes, fibrinogen, complement factors and glycoproteins<sup>34-49</sup> which explains the remarkably faster angiogenesis and de novo bone formation compared to other bone substitutes. Since NanoBone® gets substituted completely by natural bone during process of remodelling calling it 'bone augmentation material' is justified.

The role of the silica gel that disappears completely within two weeks after installation is subject to

ongoing studies (additional publication is being prepared).

## ■ Conclusion

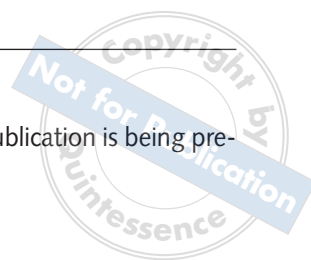
This nanostructured hydroxyapatite in a silica gel is an augmentation material that provides us with a stable and reliable implant layer within only three months after sinus floor elevation .

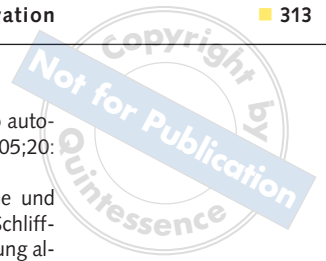
## ■ Acknowledgement

We would like to thank the following staff members for technical processing including the performance of the morphometric work: Ms H. Ahrens (MTA), Ms S. Franke (MHSc – NZ), Ms G. Hall (MTA), Dr. rer. nat. S. Lenz.

## ■ References

1. Gerber T, Holzhüter G, Götz W, Bienengraber V, Henkel K-O, Rumpel E. Nanostructuring of biomaterials – A pathway to bone grafting substitute. *Eur J Trauma* 2006;32:132-140.
2. Tatum OH. Maxillary sinus grafting for endosseous implants. Annual Meeting of the Alabama Implant Study Group: Birmingham, USA, 1977.
3. Boyne PJ, James RA. Grafting of the maxillary sinus floor with autogenous marrow and bone. *J Oral Surg* 1980;38: 613-616.
4. Wolf E. Technovit® 9100 NEU: Polymerisationssystem für die Einbettung von mineralisiertem Gewebe und Weichgewebe zur histologischen, immun- und enzymhistochemischen Untersuchung einschließlich In-situ-Hybridisierung. Heraeus Kulzer, Hanau 2001.
5. Wolf E, Röser K, Hahn M, Welkerling H, Delling G. Enzyme and immunohistochemistry on undecalcified bone and bone marrow biopsies after embedding in plastic: a new embedding method for routine application. *Virchows Archiv A Pathol Anat Histopathol* 1992;420:17-24.
6. Burkhardt R. Farbatlas der klinischen Histopathologie von Knochenmark und Knochen. Berlin: Springer, 1970.
7. Schenk R, Olah A, Herrmann W. Preparation of calcified tissues for light microscopy: In: Dickson G (ed). *Methods of Calcified Tissue Preparation*. Amsterdam – New York – Oxford: Elsevier, 1984:1-56.
8. Donath K. Preparation of histologic sections by the cutting-grinding technique for hard tissue and other material not suitable to be sectioned by routine methods – Equipment and methodical performance. Norderstedt: Publication Exakt-Kulzer, 1995.
9. Donath K. Die Trenn-Dünnschliff-Technik zur Herstellung histologischer Präparate von nicht schneidbaren Geweben und Materialien. *Der Präparator* 1988;34:197-206.
10. Parfitt AM, Drezner MK, Glorieux FH, Kanis JA, Malluche H, Meunier PJ, et al. Bone histomorphometry: standardization of nomenclature, symbols, and units. Report of the ASBMR Histomorphometry Nomenclature Committee. *J Bone Min Res* 1987;2:595-610.





11. Merz W. Die Streckenmessung an gerichteten Strukturen im Mikroskop und ihre Anwendung zur Bestimmung von Oberflächen-Volumen-Relationen im Knochengewebe. *Mikroskopie* 1967;22:132-142.
12. Lekholm U, Zarb G. Kieferanatomie. In: Brånemark I, Zarb G, Albrektson T (eds). *Gewebeintegrierter Zahnersatz*. Berlin: Quintessenz, 1985:198.
13. Schenk R, Willenegger H. Zum histologischen Bild der sogenannten Primärheilung der Knochenkompakta nach experimentellen Osteotomien am Hund. *Separatum Experientia* 1963;19:593-595.
14. Schenk R, Willenegger H. Zur Histologie der primären Knochenheilung. *Langenbecks Arch Klin Chir Ver Dtsch Z Chir* 1964;308:440-452.
15. Von Arx T, Hardt N, Wallkamm B, Kurt B. Die TIME-Technik: Lokale Osteoplastik zur Alveolarkammaugmentation – Auswertung und Ergebnisse der ersten 15 Fälle. *Implantologie* 1996;4:33-48.
16. Von Arx T, Cochran DL, Schenk RK, Buser D. Evaluation of a prototype trilayer membrane (PTLM) for lateral ridge augmentation: an experimental study in the canine mandible. *Int J Oral Maxillofac Surg* 2002;31:190-199.
17. Buser D, Ingimarsson S, Dula K, Lussi A, Hirt HP, Belser UC. Long-term stability of osseointegrated implants in augmented bone: A 5-year prospective study in partially edentulous patients. *Int J Periodontics Restorative Dent* 2002;22:108-117.
18. Buser D. Aus der Gefahren-Zone in die Komfort-Zone (Vortrag). EAO-Tagung: München, 2005.
19. Ewers R, Kasperk C, Simons B. Biologisches Knochenimplantat aus Meeresalgen. *Zahnärztl Praxis* 1987;38:319-324.
20. György S, Huys L, Coulthard P, Maiorana C, Garagiola U, Barabas J, et al. A prospective multicenter randomized clinical trial of autogenous bone versus  $\beta$ -tricalcium-phosphate graft alone for bilateral sinus elevation. Histologic and histomorphometric evaluation. *Int J Oral Maxillofac Implants* 2005;20:371-381.
21. Hallman M, Sennerby L, Lundgren S. A clinical and histologic evaluation of implant integration in the posterior maxilla after sinus floor augmentation with autogenous bone, bovine hydroxyapatite or a 20:80 mixture. *Int J Oral Maxillofac Implants* 2002;17:635-643.
22. Härle F. Augmentation with hydroxylapatite and vestibuloplasty in the atrophic maxilla with a flabby ridge. *J Maxillofac Surg* 1985;13:209-212.
23. Haessler D, Fürst U, Foitzik C. Implantatversorgung des teilbezahnten Gebisses nach Extension und Augmentation des Kieferkammes durch freie autogene Knochen transplantation. *Quintessenz* 1994;45:645-652.
24. Maas W, Bienengraeber V, Wolf E. Sicher augmentieren – Split-mouth-Fallstudie zur Augmentation mittelgroßer Knochendefekte. *Implantologie Journal* 2006;5:40-44.
25. Terheyden H. Knochenzüchtung – geht das? (Vortrag). Jahrestagung DGI, München, 2007.
26. Valentini P, Abensur D, Wenz B, Peetz M, Schenk R. Sinus grafting with porous bone mineral (Bio-Oss) for implant placement: A 5-year study on 15 patients. *Int J Periodontics Restorative Dent* 2000;20:245-253.
27. Wallace SS, Froum SJ, Cho SC, Elian N, Monteiro D, Kim BS, et al. Sinus augmentation utilizing anorganic bovine bone (BioOss) with absorbable and nonabsorbable membranes placed over the lateral window: Histomorphometric and clinical analysis. *Int J Periodontics Restorative Dent* 2005;25:551-559.
28. Zijdeveld SA, Zerbo IR, van den Bergh JP, Schulten EA, ten Bruggenkate CM. Maxillary sinus floor augmentation using  $\beta$ -tricalcium phosphate (Cerasorb) alone compared to autogenous bone grafts. *Int J Oral Maxillofac Implants* 2005;20:432-440.
29. Röser K, Donath K, Schnettler R. Histopathologische und histochemische Untersuchung an unentkalkten Schliffpräparaten zur Knochendefektheilung unter Verwendung allogener Transplantate und poröser Hydroxylapatitkeramik-Implantate. *Osteosynthese International* 1994;2:124-134.
30. Osborn JF. Die enossale Implantation von Hydroxylapatitkeramik unter Verwendung des Fibrinklebesystems. *Dtsch Zahnärztl Z* 1983;38:956-958.
31. Donath K, Hormann K, Kirsch A. Welchen Einfluss hat Hydroxylapatitkeramik auf die Knochenbildung? *Dtsch Z Mund Kiefer Gesichtschir* 1985;9:438-440.
32. Schenk R, Willenegger H. Zur Histologie der primären Knochenheilung. Modifikation und Grenzen der Spaltheilung in Abhängigkeit von der Defektgröße. *Unfallheilkunde* 1977;80:155-160.
33. Schenk R. Die Histologie der primären Knochenheilung im Lichte neuer Konzeptionen über den Knochenumbau. *Unfallheilkunde* 1978;81:219-227.
34. Friedenstein A (Hrsg). *Determined and Inducible Osteogenic Precursor Cells*. Amsterdam: Elsevier, 1973.
35. Friedenstein A. Precursor cells of mechanocytes. *Int Rev Cytol* 1976;47:327-359.
36. Friedenstein AJ, Chailakhyan RK, Gerasimov UV. Bone marrow osteogenic stem cells: in vitro cultivation and transplantation in diffusion chambers. *Cell Tissue Kinet* 1987;20:263-272.
37. Owen M. The origin of bone cells in the postnatal organism. *Arthritis & Rheumatism* 1980;23:1073-1080.
38. Owen M, Cave J, Joyner C. Clonal analysis in vitro of osteogenic differentiation of marrow CFU-F. *J Cell Sci* 1987;87:731-738.
39. Donath K, Laaß M, Günzl H-J. The histopathology of different foreign-body reactions in oral soft tissue and bone tissue. *Virchows Archiv A Pathol Anat Histopathol* 1992;420:131-137.
40. Vroman L, Adams AL, Klings M. Interactions among human blood proteins at interfaces. *Federation Proceedings* 1971;30:1494-1502.
41. Hartwig BA, Lohman RE, Hench LL. Morphology of polypeptide adsorption on ceramic substrates. *Am Ceram Soc Bull* 1973;52:430.
42. Van Oss CJ. Phagocytosis as a surface phenomenon. *Ann Rev Microbiol* 1978;32:19-39.
43. Klein CPAT, de Groot K, Vermeiden JPW, van Kamp G. Interaction of some serum proteins with hydroxylapatite and other materials. *J Biomed Mater Res* 1980;14:705-712.
44. Chambers IJ. The response of the macrophage to foreign material: In: Williams DF (ed): *Fundamental Aspects of Biocompatibility*. Boca Raton Florida: CRC Press, 1981:145-158.
45. Hoffman AS. Principles governing biomolecule interactions at foreign interfaces. *J Biomed Mater Res* 1974;8:77-83.
46. Taylor AC. Adhesion of cells to surfaces: In: Manly RS (ed): *Adhesion in Biological Systems*. New York: Academic Press, 1970:51-71.
47. Sakamoto S, Sakamoto M. Bone collagenase, osteoblasts and cell-mediated bone resorption. In: Peck W (ed). *Bone and Mineral Research*. Amsterdam – New York – Oxford: Elsevier, 1986:49-102.
48. Frost H. *The Bone Dynamics in Osteoporosis and Osteomalacia*. Springfield, USA: Thomas, 1966.
49. Rassmussen H, Bordier P. *The physiological and cellular basis of metabolic bone disease*. Baltimore: Williams & Wilkins, 1974.